

## DOES ACCRETION CEASE WHEN A STAR APPROACHES BREAKUP?

ROBERT POPHAM AND RAMESH NARAYAN

Steward Observatory, University of Arizona, Tucson, AZ 85721

Received 1990 June 6; accepted 1990 September 19

### ABSTRACT

We investigate whether disk accretion can continue as the accreted angular momentum spins the central star to near breakup. We model a steady-state thin accretion disk around a uniformly-rotating unmagnetized star using a two-dimensional fluid with a polytropic equation of state and  $\alpha$ -viscosity. We explicitly include gradients in the radial velocity and the pressure and numerically solve for the angular velocity profile. We treat the specific angular momentum,  $j$ , added to the star as an eigenvalue of the problem that is determined through the boundary conditions. We find that there is a mapping between  $j$  and the stellar rotation rate,  $\Omega_*$ , with the following properties. When  $\Omega_*$  is somewhat less than the breakup rotation rate of the star,  $\Omega_{\max}$ , we find a class of solutions where the angular velocity of the disk attains a maximum close to the star and then decreases rapidly in a boundary layer to match  $\Omega_*$ . For a thin disk with thickness  $\sim 0.01$  times the radius and  $\alpha = 0.1$ , the radial flow of the accreting material briefly becomes supersonic in the boundary layer before being decelerated in a radial shock. For a thicker disk (thickness  $\sim 0.1$  times radius) with much smaller viscosity ( $\alpha = 0.0001$ ), the flow is subsonic throughout. In either case,  $j$  is almost independent of  $\Omega_*$  and is approximately equal to the Keplerian specific angular momentum at the stellar surface. This agrees with the standard picture of angular momentum transport in thin disks. However, if  $\Omega_*$  is near breakup, then we find a second class of solutions where the disk angular velocity has no maximum at all but increases monotonically all the way down to the stellar surface; the flow remains subsonic for all choices of disk thickness and  $\alpha$ . For these solutions,  $j$  decreases extremely rapidly with increasing  $\Omega_*$  and even takes on fairly large negative values. Because of this, the spin-up of an accreting star slows down and eventually stops at a rotation rate near breakup. Beyond this point, the star can continue to accrete any amount of matter without actually breaking up. This result has applications in star formation and in the theory of cataclysmic variables. It also eliminates one of the objections to the accretion-induced collapse scenario for the formation of low-mass binary neutron stars.

*Subject headings:* accretion — stars: accretion — stars: binaries — stars: formation — stars: rotation — stars: white dwarfs

### 1. INTRODUCTION

Accretion disks deliver both mass and angular momentum to their central accreting stars (see Pringle 1981 for a review). In the case of accreting magnetized stars such as the binary X-ray pulsars (see Lewin & van den Heuvel 1984 and references therein), one sees direct evidence for the addition of angular momentum in the spin-up of the stars. A feature of these systems is that there is a maximum rotation rate to which the stars are spun up. Once the star has achieved this rotation, mass accretion can still continue but there is no additional spin-up. This phenomenon has been modeled by Ghosh & Lamb (1979) who showed that there is a cancellation between the positive torque due to the angular momentum carried in by the accreting material and a negative torque due to the interaction between the stellar magnetic field and the fluid in the accretion disk. The existence of negative feedback from the magnetic torque thus ensures that an accreting magnetized star asymptotically approaches, but does not exceed, a stable “equilibrium” rotation rate.

The situation is less clear in the case of accretion by an *unmagnetized* object. In this case it is generally assumed that the central star receives specific angular momentum from the disk at a rate corresponding approximately to the Keplerian angular momentum at the surface of the star. Further, in the standard picture, there is no opposing torque or negative feedback mechanism. One therefore expects that if accretion were

to continue long enough the star would be spun up to and possibly even beyond its maximum allowed rotation rate,  $\Omega_{\max}$ , the so-called “breakup” rate, where the equatorial centrifugal force just balances the force of gravity. What happens beyond this point is not known. Since the star is apparently unable to accept any more mass from the accretion disk, because it cannot accommodate the angular momentum that goes with it, one might imagine that either the accumulating material is ejected through a wind or via jets, or the matter builds up to form a relatively independent envelope around the central star.

The question of what happens when there is continued accretion onto an unmagnetized star close to breakup has become relevant as a result of two recent studies. Shu et al. (1988) investigated star-forming disks and argued that the central objects would be quickly spun-up to  $\Omega_{\max}$ . They proposed that such a system would then eject a wind from the circumferential cusp that forms around the rapidly spinning star. This wind may be collimated to produce the outflows that are seen in star-forming regions. In another study, we (Narayan & Popham 1989) investigated the spin history of accreting white dwarfs and found that unmagnetized white dwarfs attain  $\Omega_{\max}$  after accreting as little as  $\sim 0.1 M_{\odot}$ , assuming that there is no mass loss through nova ejection. Since white dwarfs in cataclysmic variables are thought to accrete several tenths of a solar mass during the course of their evolution, it seems likely that many of these systems should achieve a spin rate close to  $\Omega_{\max}$ . A question we were unable to answer in the earlier study,

and which we pursue in this paper, is: What does an accreting unmagnetized white dwarf, or any other unmagnetized star, do when its spin rate approaches  $\Omega_{\max}$ ?

This question is particularly interesting in the case of massive accreting white dwarfs. In these objects, the angular momentum corresponding to breakup,  $J_{\max}$ , decreases with increasing mass,  $M$  (e.g., Hachisu 1986), because of the steep inverse mass-radius relation. This means that once the white dwarf has achieved a spin rate  $\sim \Omega_{\max}$ , it must actually lose angular momentum in order to accrete any more mass. At first glance, it appears impossible for an accretion disk to remove angular momentum from a star while at the same time supplying mass to it—as we mentioned above, the current wisdom is that there is a certain fixed amount of positive angular momentum that is associated with any accreted matter. The main purpose of the present paper is to demonstrate that disks can indeed remove angular momentum from the accreting object.

We construct here steady axisymmetric accretion disk models where we allow the specific angular momentum,  $j$ , added to the central star to be a free parameter. We show that  $j$  behaves like an eigenvalue that is self-consistently determined by the various boundary conditions that the disk must satisfy. The most important of the boundary conditions is that the rotation rate of the star,  $\Omega_*$ , should match that of the disk at the boundary between the two. As a consequence of this condition we find that there is a precise mapping between  $\Omega_*$  and  $j$ . This mapping is such that  $j$  is approximately equal to the Keplerian specific angular momentum at the equator of the star whenever  $\Omega_*$  is somewhat less than  $\Omega_{\max}$ . This result is in agreement with conventional wisdom. However, we find that  $j$  becomes much smaller, and even takes on (quite large) negative values, when  $\Omega_*$  is close to  $\Omega_{\max}$ . Because of the existence of such negative  $j$  solutions, there is a natural negative feedback mechanism, and the central star can continue to accrete any amount of matter even when it approaches  $\Omega_{\max}$ . In this sense, accretion onto an unmagnetized star behaves exactly as in the magnetized case; the only difference is that the “equilibrium” rotation rate here is of order  $\Omega_{\max}$ , whereas in the magnetized systems it is determined by the Keplerian  $\Omega$  at the magnetospheric radius.

Our results confirm previous work by Pringle (1989) who argued that, even when a star is rotating exactly at breakup, accretion is not prevented. In Pringle’s view only a star with  $\Omega_* > \Omega_{\max}$  can stop accreting. The present work advances these ideas in two ways. First, we construct models that reveal the explicit connection between the stellar rotation rate  $\Omega_*$  and the accreted specific angular momentum  $j$ . Thus, in a sense, we have quantified Pringle’s argument. Second, we show that solutions with negative  $j$  are possible. Thus, a star can lose angular momentum—quite a lot of it if necessary—while at the same time continuing to accrete. We are not aware of any previous work that anticipated this result.

After we had completed this study, we discovered that Paczyński (1990) had independently carried out a similar investigation. Although using a somewhat different approach, Paczyński agrees with most of our conclusions. In particular, he too finds that accretion is not inhibited when a star approaches breakup.

## 2. THEORY

### 2.1. Fluid Model

A key feature of our approach is that we treat the accretion disk, the boundary layer and the accreting star all as a single

fluid system, described by the same set of equations. In order to simplify the analysis, we further assume that the fluid properties can be integrated in the vertical direction, i.e., the direction parallel to the rotation axis, so that the system can be described in terms of an effective two-dimensional fluid. This approximation is routinely made in the theory of thin accretion disks and is clearly valid in the outer parts of our model. It is less clear that the approximation is allowed in the central regions. However, as we show below, the model does represent the star reasonably well, at least near the disk-star interface, and so there is no serious error from this assumption. In any case, we feel that the two-dimensional approximation will not affect the qualitative features of our results.

Assuming that the fluid attains an axisymmetric steady state, its surface density profile is described by a function  $\Sigma(R)$ , where  $R$  is the radial distance from the center of the star. We use the equatorial radius of the star as our unit of length so that  $R = 1$  represents the equatorial boundary of the star. As we discuss below, the exact position of the boundary is hard to locate since there is a smooth transition from the star to the disk. We use a particularly simple definition for the edge of the star, viz., that the vertical half-thickness is  $H = 0.1$  at  $R = 1$  (see eq. [18] below). We are confident that the main results are not influenced by this choice. We take the outer edge of the disk at some large radius, typically  $R_{\text{out}} = 100$ . We have verified that the results are quite insensitive to the choice of  $R_{\text{out}}$ .

The motion of the fluid is described by an angular velocity profile,  $\Omega(R)$ , and a radial velocity,  $v_R(R)$ . The latter is taken to be positive when pointed outward and is therefore negative for accretion. We take our unit of frequency to be such that the Keplerian angular velocity,  $\Omega_K(R)$ , is unity at  $R = 1$ , i.e.,

$$\Omega_K(R) = R^{-3/2}. \quad (1)$$

We assume that the two-dimensional fluid satisfies a polytropic equation of state,

$$P = K\Sigma^\gamma, \quad (2)$$

where  $P$  is the height-integrated pressure, and  $K$  and  $\gamma$  are constants. In principle, we could solve our equations for any choice of  $\gamma$ . However, in an attempt to be realistic we have selected  $\gamma = 2$  for most of our computations. As we show in Appendix A, this produces the best match between our results and those of a standard thin accretion disk around a white dwarf.

For a steady accretion rate  $\dot{M}$ , mass conservation gives

$$\dot{M} = -2\pi R v_R \Sigma. \quad (3)$$

Using this, the sound speed,  $c_s$ , of the fluid may be written as

$$c_s^2 = \frac{dP}{d\Sigma} = \gamma K \Sigma^{\gamma-1} = C_0^2 (R |v_R|)^{1-\gamma}. \quad (4)$$

The parameter  $C_0$  describes a combination of  $\dot{M}$  and the fluid constants  $K$  and  $\gamma$ . In our calculations we usually selected  $C_0$  such that the sound speed at the outer edge was a fixed fraction  $X$  of the local Keplerian velocity, i.e.,

$$c_s(R_{\text{out}}) = X R_{\text{out}}^{-1/2}. \quad (5)$$

Since a typical cataclysmic variable has  $c_s/\Omega_K R \sim 0.01$  at the outer edge (see Frank, King, & Raine 1985), we set  $X = 0.01$  in most of our calculations. As we see from equation (13) below,  $X$  is a measure of the relative thickness of the disk.

## 2.2. Equations of Motion

The continuity equation has been absorbed into our mapping between  $c_s$  and  $v_R$  in equation (4), and we do not need an energy equation because of the polytropic assumption. Therefore, the dynamics are completely described by the two components of the equation of motion.

In steady state, the radial equation of motion gives

$$v_R \frac{dv_R}{dR} = (\Omega^2 - \Omega_K^2)R - \frac{1}{\Sigma} \frac{dP}{dR}, \quad (6)$$

which may be rewritten as

$$\frac{dv_R}{dR} = \frac{v_R[(\Omega_K^2 - \Omega^2)R^2 - c_s^2]}{R(c_s^2 - v_R^2)}. \quad (7)$$

The form of the denominator alerts us to the possibility of obtaining a sonic point in the solution. By including pressure terms in the radial equation, we have thus gone beyond the standard theory of thin accretion disks; in fact, an equation similar to equation (7) is used in the theory of so-called "slim" accretion disks (Abramowicz et al. 1988; see also Paczyński & Bisnovatyi-Kogan 1981; Muchotrzeb & Paczyński 1982).

Next we obtain a differential equation for  $\Omega$  by considering the tangential equation of motion. Let the disk transport angular momentum inward at a steady rate  $\dot{J}$ , and let us define

$$j \equiv \dot{J}/\dot{M}. \quad (8)$$

By our choice of units,  $j$  is expressed in units of the Keplerian angular momentum at the defined edge of the star. Going back to our discussion in § 1, the usual assumption is that  $j \sim 1$ , regardless of the rotation of the star, for disks around unmagnetized stars. We avoid this assumption and treat  $j$  as an adjustable parameter—an eigenvalue—whose value is determined by the boundary conditions.

Consider now the angular momentum flow across some radius  $R$  in the system. The accreting fluid carries angular momentum inwards at the rate  $\dot{M}\Omega R^2$ . At the same time, there is an outward flux of angular momentum because of the viscous stress. If the kinematic coefficient of viscosity is  $\nu$ , then we have the following relation,

$$\dot{M}\Omega R^2 + 2\pi R^2 \nu \Sigma \frac{d\Omega}{dR} = \dot{J}. \quad (9)$$

Substituting equation (3) for  $\Sigma$  and using equation (8), this can be rewritten as

$$\frac{d\Omega}{dR} = \frac{v_R}{\nu} \left( \Omega - \frac{j}{R^2} \right). \quad (10)$$

For the viscosity, we use the standard  $\alpha$ -prescription of Shakura & Sunyaev (1973), which we write in the form

$$\nu(R) = \frac{\alpha c_s^2(R)}{\Omega_K(R)} = \alpha R^{3/2} c_s^2(R). \quad (11)$$

We assumed  $\alpha = 0.1$  in most of the calculations.

The differential equations (7) and (10), coupled with the relations (4) and (11), allow us to solve for  $v_R(R)$ ,  $\Omega(R)$ , and  $c_s(R)$ , given appropriate boundary conditions. The equations are, however, very stiff and cannot be integrated by any of the standard initial-value integrators. All our results were obtained using a relaxation method (see, e.g., Press et al. 1986). Apart from overcoming the stiffness of the equations, the relaxation

method was also particularly convenient for handling sonic points in equation (7).

A derived quantity of particular interest is the thickness of the disk,  $H(R)$ . To calculate this, we obviously need to abandon the two-dimensional approximation and make some assumption regarding the three-dimensional properties of the fluid. This question is discussed in Appendix A, where we show that, for a polytropic fluid with a particular choice of polytropic indices ( $\gamma = 2, \gamma_3 = 3$ ), we have the relation

$$\frac{H}{R} = \sqrt{2} \frac{c_s}{\Omega_K R} = \sqrt{2} R^{1/2} c_s(R). \quad (12)$$

The form of the relation between  $H$  and  $c_s$  is robust, but the particular coefficient,  $\sqrt{2}$ , is not to be taken seriously since it depends on somewhat arbitrary assumptions. A relation very similar to equation (12) was used by Papaloizou & Stanley (1986).

## 2.3. Outer Boundary Conditions

Equations (5) and (12) combine to give one of the boundary conditions at the outer edge, viz.,

$$\frac{H(R_{\text{out}})}{R_{\text{out}}} = \sqrt{2} X. \quad (13)$$

For our standard choice,  $X = 0.01$ , the disk is clearly quite thin at the outside. Moreover, for our value of  $\gamma = 2$ , we have  $H/R \propto R^{1/8}$  (see Appendix A) and so we are assured that, as we move in to smaller radii, the disk remains thin all the way down to the transition zone near the star.

As a second boundary condition at the outer edge, we set

$$\Omega(R_{\text{out}}) = \Omega_K(R_{\text{out}}) = R_{\text{out}}^{-3/2}, \quad (14)$$

so that the disk is constrained to have the rotation rate appropriate to a standard thin disk. In practice, it turned out that the solutions are not sensitive to the choice of  $\Omega(R_{\text{out}})$ . If a somewhat different choice was made for  $\Omega(R_{\text{out}})$ , the solution would settle down to a near-Keplerian  $\Omega(R)$  within a short distance from  $R_{\text{out}}$  and then track  $\Omega_K(R)$  except in the region close to the star at  $R \sim 1$ .

Because of the above comment,  $\Omega(R)$  is quite accurately Keplerian near the outer edge. Coupled with equations (4), (10), and (11), this permits us to calculate the infall velocity at the outer edge as well as the constant  $C_0$ ,

$$v_R = -\frac{3}{2} \frac{\nu}{R} \frac{1}{(1 - j/R^{1/2})}, \quad (15)$$

$$C_0 = c_s(-Rv_R)^{(\gamma-1)/2} = X^\gamma R^{-\gamma/2} \left( \frac{3\alpha R^{3/2}/2}{1 - j/R^{1/2}} \right)^{(\gamma-1)/2}. \quad (16)$$

Note that the radial velocity is quite subsonic at the outer edge of the disk.

## 2.4. Inner Boundary Conditions

One obvious condition here is that  $\Omega(R)$  should equal the rotation rate of the star,  $\Omega_*$ , at  $R = 1$ , i.e.

$$\Omega(R) = \Omega_*, \quad R = 1. \quad (17)$$

Presumably, in a good solution,  $\Omega(R)$  will be essentially independent of  $R$  and remain equal to  $\Omega_*$  for  $R < 1$ , in order to represent the interior of a rigidly rotating star. This then brings up a rather subtle point: how do we define the exact location of



the boundary between the disk and the star? Unfortunately, there appears to be no unique answer to this since we are treating the disk and the star as a single fluid system.

For the sake of simplicity, we have taken the edge of the star to be *defined* as that radius where the relative thickness reaches a particular (arbitrarily chosen) value, viz.,

$$H(R) = 0.1, \quad R = 1. \quad (18)$$

The particular value, 0.1, was chosen so as to be larger than the accretion disk thickness by a reasonable factor. Obviously, we do not claim that the point at which  $H/R = 0.1$  represents the true stellar edge. We are merely selecting it as a convenient fiducial marker that is likely to be reasonably close to any other better-defined stellar edge. See § 3.3 for further discussion of this point.

### 3. RESULTS

#### 3.1. Two Solution Branches

By numerical solution of the equations for the particular choice of parameters,  $\gamma = 2$ ,  $X = 0.01$ ,  $\alpha = 0.1$ , we discovered two distinct branches of solutions with the following characteristics:

1. *Supersonic Solutions.*—These solutions have the characteristics of standard thin disks at large  $R$ . However, close to the star, they have a sonic radius,  $R_s$ , where the conditions  $c_s = |v_R| = (\Omega_K^2 - \Omega^2)^{1/2} R$  are satisfied (see eq. [7]). For  $R < R_s$ , the flow becomes supersonic. In order to match on to the star, the supersonic regime is terminated in a radial standing shock at a shock radius,  $R_{sh}$ , inside of which the flow adopts the character of a settling solution and merges with the star. Solutions in this branch usually correspond to stellar rotation rates  $\Omega_*$  somewhat below unity. The run of  $\Omega$ ,  $v_R$  and  $H$  of a typical solution of this type is shown in Figure 1. This solution corresponds to  $j = 1.004$ ,  $\Omega_* = 0.5796$ , and has  $R_s = 1.00777$ ,  $R_{sh} = 1.00763$ . Supersonic solutions can match on to the star only if  $R_s \geq 1$ . Because of this requirement, we find that they exist only for  $j > 1.0005$  (for the assumed  $\gamma$ ,  $X$ ,  $\alpha$ ).

2. *Subsonic Solutions.*—These solutions again behave like thin disks at large  $R$  but remain subsonic all the way into the star. They make a fairly abrupt (but continuous) transition from a Keplerian rotation profile,  $\Omega(R) \simeq \Omega_K(R)$ , to the constant stellar rotation,  $\Omega(R) = \Omega_*$ , at a radius outside our defined stellar edge. These solutions usually correspond to  $\Omega_*$  close to unity (the breakup stellar rotation). Figure 2 shows a typical member of this solution type and corresponds to  $j = 1.004$ ,  $\Omega_* = 0.9142$ . Subsonic solutions exist for a range of values of  $j$ , including quite large negative values.

The two solutions shown in Figures 1 and 2 both have the same eigenvalue  $j$  and satisfy the same boundary conditions at  $R = 1$  and  $R = R_{out}$ , but have very different stellar rotations,  $\Omega_*$ . The topological relation between these two branches is revealed by relaxing our inner boundary condition, equation (18), and considering instead a range of values for the height  $H(R = 1)$  at the stellar edge. We then obtain Figure 3, where we show  $\Omega_*$  as a function of  $H(R = 1)$  for the two solution branches. We find that the two branches meet at a mathematical cusp. The solution corresponding to the tip of the cusp may be interpreted either as the last subsonic solution, that barely avoids the sonic point, or as the first supersonic solution, with an infinitesimally weak shock immediately following the sonic point. This particular solution has the smallest allowed value of  $H(R = 1)$  for the given value of  $j$ . As we move away from the

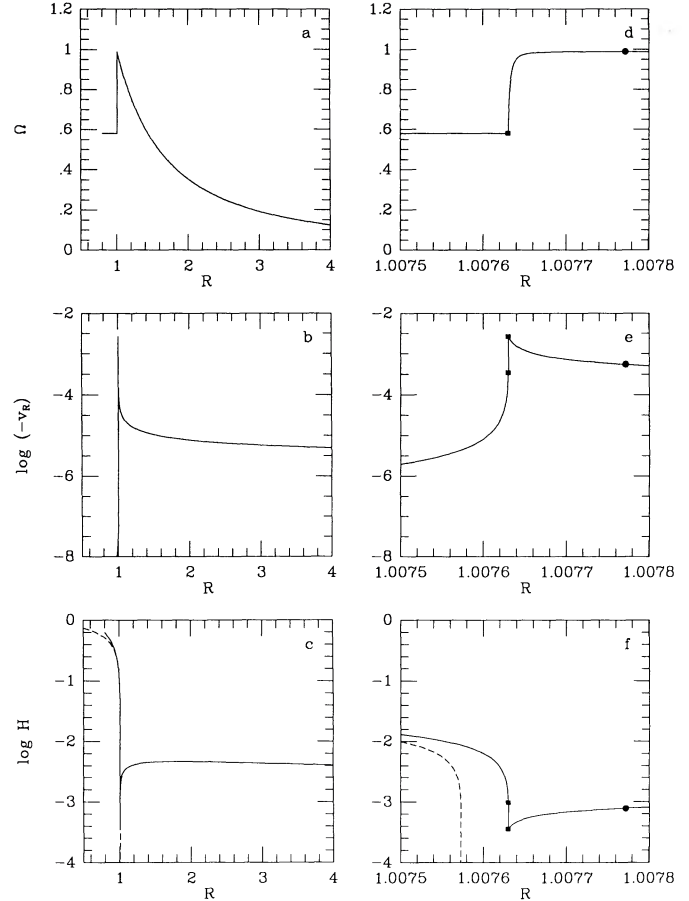


FIG. 1.—The radial dependence of  $\Omega$ ,  $v_R$ , and  $H$  for a supersonic disk solution corresponding to  $X = 0.01$ ,  $\alpha = 0.1$ ,  $R_{out} = 100$ ,  $j = 1.004$ , and  $\Omega_* = 0.5796$ . (a)  $\Omega$  vs.  $R$ ; note the abrupt decrease of  $\Omega$  in a boundary layer from a near-Keplerian value to  $\Omega_*$ . (b)  $v_R$  vs.  $R$ ;  $|v_R|$  increases slowly in the Keplerian part of the disk, rises rapidly in the supersonic region, peaks at the shock position, and finally decreases rapidly as the material settles onto the star. (c)  $H$  vs.  $R$ ; the disk height decreases gradually in the Keplerian disk, then more rapidly to reach a minimum at the shock position; in the settling region the height increases as the disk joins the star; the dashed line shows  $H$  vs.  $R$  for a uniformly rotating star in a point-mass potential with the same  $\Omega_*$ . (d)–(f) Show the same quantities as (a)–(c), but with the radial scale expanded to show the structure of the boundary layer; the circles show the position of the sonic point and the squares show the shock. The two squares used for  $v_R$  and  $H$  show the values on either side of the shock;  $\Omega$  is continuous across the shock, but  $d\Omega/dR$  is not.

cusp point in Figure 3 along the supersonic branch, the solutions have an increasingly larger separation between  $R_s$  and  $R_{sh}$ , the shock increases in strength, and the stellar rotation rate  $\Omega_*$  decreases. In fact, even solutions with negative  $\Omega_*$  (backward-spinning star) are possible.

#### 3.2. Spin History of an Accreting Star

Figure 4 is similar to Figure 3, but shows the supersonic and subsonic branches for a range of values of  $j$ . Both branches exist for  $j > 1.0005$ , but only the subsonic branch is possible for  $j < 1.0005$ .

The dashed line in Figure 4 corresponds to our boundary condition,  $H(R = 1) = 0.1$  (eq. [18]). An accreting star that begins with no rotation traverses this line starting at  $\Omega_* = 0$  and moving to the right. At each value of  $\Omega_*$ , there is a unique

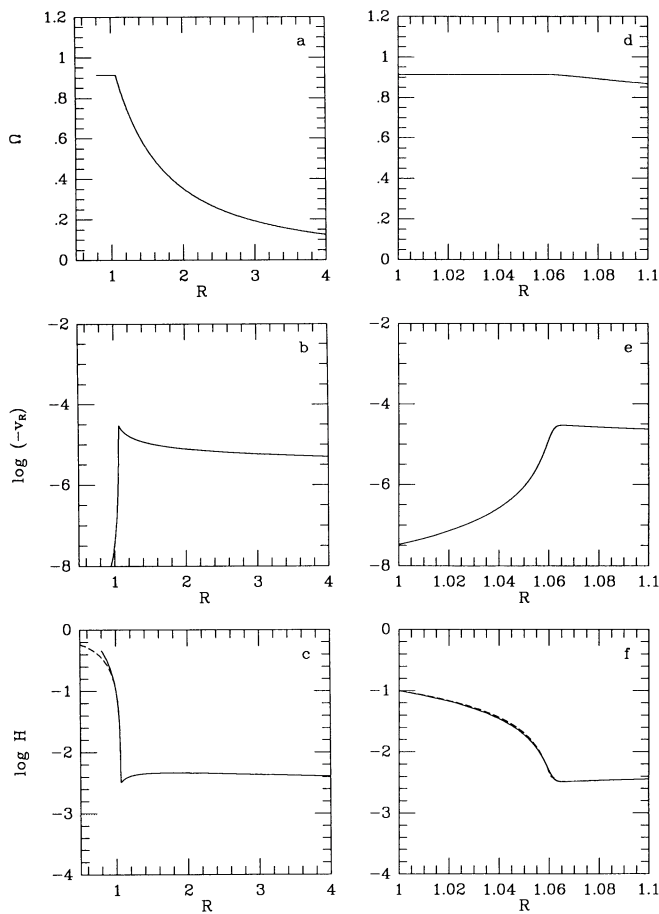


FIG. 2.—The radial dependence of  $\Omega$ ,  $v_R$ , and  $H$  for a subsonic disk solution corresponding to  $X = 0.01$ ,  $\alpha = 0.1$ ,  $R_{\text{out}} = 100$ ,  $j = 1.004$ , and  $\Omega_* = 0.9142$ . (a)  $\Omega$  vs.  $R$ ; the angular velocity is nearly Keplerian until it reaches  $\Omega_*$ , and then stays nearly constant in to the stellar surface. (b)  $v_R$  vs.  $R$ ;  $|v_R|$  reaches a maximum close to the star and decreases in to the stellar surface, but both the maximum and subsequent decrease are far less abrupt than in the supersonic solution shown in Fig. 1. (c)  $H$  vs.  $R$ ; the disk height reaches a minimum and then increases as the disk meets the star; again the minimum and subsequent rise are less abrupt than their supersonic counterparts; the dashed line shows  $H$  vs.  $R$  for a uniformly rotating star in a point-mass potential with the same  $\Omega_*$ . (d)–(f)  $\Omega$ ,  $v_R$ , and  $H$  in the region close to the stellar surface. Unlike the supersonic disk in Fig. 1, all three quantities and their gradients are continuous.

value of  $j$  of the accretion disk, i.e., there is a unique rate at which the star accretes angular momentum. The mapping between  $\Omega_*$  and  $j$  is shown in Figure 5. For most of the range of  $\Omega_*$ , the flow corresponds to the supersonic branch, and the value of  $j$  is relatively insensitive to  $\Omega_*$ . However, when as a result of spin-up  $\Omega_*$  exceeds 0.914, the solution switches from the supersonic to the subsonic branch. Immediately, the nature of the  $\Omega_*$  versus  $j$  mapping also changes dramatically. Now the curves corresponding to different  $j$  crowd together in Figure 4 and, consequently, a small increase in  $\Omega_*$  causes a large decrease in  $j$ .

The fact that  $j$  plummets to large negative values as  $\Omega_*$  approaches unity implies that any star will be able to continue accreting indefinitely without ever encountering an angular momentum barrier. Consider, for instance, the situation we mentioned in § 1, namely, accretion on to an unmagnetized massive white dwarf. This is a case where the maximum

angular momentum  $J_{\text{max}}$  of the star decreases as its mass  $M$  increases. This means that when such a star approaches the critical rotation it will require a disk with negative  $j$  in order to continue to accrete. From Hachisu's (1986) results we estimate that a white dwarf close to the Chandrasekhar limit may need  $j \sim -1$ . As we have shown above (Fig. 5), subsonic solutions with negative  $j$  are available and the star can indeed continue accreting.

Figure 6 shows in detail the solution corresponding to  $j = -10$ . It will be noted that this solution is rather similar to the subsonic solution with  $j = 1.004$  shown in Figure 2. Thus, the negative  $j$  solutions are not different or peculiar in any way. They are quite reasonable solutions which may be expected to occur whenever the conditions require them.

### 3.3. Location of the Stellar Edge

A somewhat unsatisfactory feature of our analysis is that we are unable to identify uniquely the boundary between the star and the disk. Figures 1, 2, and 6 show that our particular choice (based on eq. [18]) is not unreasonable since (1)  $\Omega(R)$  is very nearly constant interior to our defined boundary at  $R = 1$  and varies rapidly outside it, (2) the vertical thickness of the fluid increases rapidly interior to  $R = 1$  as it would in a star, and (3) the infall velocity  $|v_R|$  decreases rapidly for  $R < 1$ . All these criteria suggest that the “real” stellar edge is not very far from our defined edge.

In order to demonstrate that the fluid at  $R < 1$  does represent the star fairly well, we show by dashed lines in Figures 1, 2, 6, and 7, the shape of a rigidly rotating polytropic star in a point-mass potential with a rotation rate  $\Omega_*$ . We see that the  $H(R)$  profiles obtained from our solutions track those of the model stars reasonably well. (The small mismatch in Fig. 1f occurs because the “star” in our solution spins faster in its outer layers.) Despite the satisfactory agreement between our solutions and the model stars, the smooth transition from disk to star makes it difficult to identify uniquely the radius of the star.

This uncertainty regarding the stellar radius in turn makes it difficult to answer the simple question: what is the ratio of the maximum or “equilibrium” rotation,  $(\Omega_*)_{\text{max}}$ , achieved by an accreting star to its breakup rotation,  $\Omega_{\text{max}}$ ? We have expressed  $\Omega_*$  in terms of the Keplerian  $\Omega_K$  at the edge of the star, defined as the radius where  $H/R = 0.1$ . In these units, we see from Figure 6 that  $(\Omega_*)_{\text{max}} = 0.9157$  for a star that requires  $j = -10$  at equilibrium. More normally,  $j$  is probably greater than 0 at equilibrium and  $(\Omega_*)_{\text{max}} \simeq 0.9145$ . An isolated uniformly rotating polytropic star with  $H = 0.1$  at  $R = 1$  breaks up if  $\Omega_* > 0.9141$ . If we use this as our definition of  $\Omega_{\text{max}}$  (see Paczyński 1990), then we see that the cases with  $j = -10$  and 0 mentioned above are both spinning faster than breakup. Of course, the stars do not actually break up because they spin more slowly on the outside.

### 3.4. The Role of the Supersonic Solutions

In the calculations reported above, we found a sudden change in the character of the solutions, as well as in the  $j$  versus  $\Omega_*$  mapping, between the supersonic and subsonic branches. This might lead one to suspect that it is the existence of the supersonic branch that leads to the particular nature of the mapping. In fact, this turns out not to be the case.

Papaloizou & Stanley (1986) showed that supersonic flows occur in disk boundary layers only if the viscosity is high. By using a lower viscosity coefficient in the boundary layer, where

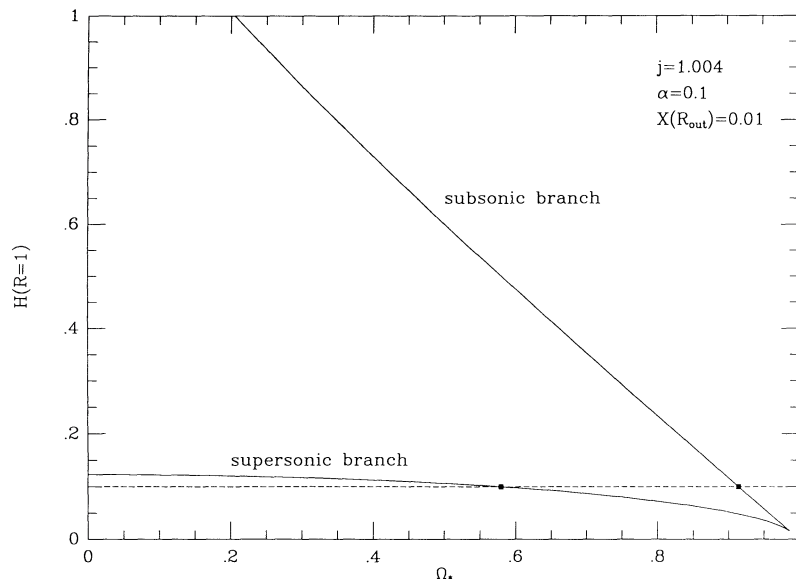


FIG. 3.—The disk height,  $H$ , at the stellar surface,  $R = 1$ , as a function of the stellar rotation rate  $\Omega_*$ , for supersonic and subsonic solutions with  $X = 0.01$ ,  $\alpha = 0.1$ ,  $R_{\text{out}} = 100$ , and  $j = 1.004$ . Note that the two physically distinct solution branches meet at a sharp cusp. Our boundary condition,  $H = 0.1$  at  $R = 1$ , corresponds to the dashed line. The solutions shown in Figs. 1 and 2 are marked by squares.

the pressure scale height becomes smaller than the disk thickness, they could find completely subsonic flows even with slowly rotating stars. Appendix B presents an analysis of our fluid equations in the region of the boundary layer which confirms this result. We find that for  $\gamma = 2$ , fully subsonic solutions should be possible if the following condition is satisfied, viz.,

$$\alpha \lesssim CX^2, \quad (19)$$

where  $X$  is defined at  $R_{\text{out}} = 100$  (see eq. [5]). The constant  $C$  is estimated to be  $\sim 0.4$  and may be up to a factor  $\sim 2$  smaller.

The calculations presented so far have used  $X = 0.01$ ,  $\alpha = 0.1$ . Since these parameters violate the above constraint by a large factor, we obtained supersonic solutions for a wide range of  $\Omega_*$ . To test this further, we have repeated our calculations for the parameter values,  $X = 0.1$ ,  $\alpha = 0.0001$ , which satisfy the constraint in equation (19). For these parameters, we do find subsonic solutions for all  $\Omega_*$ , as expected. Figure 7 shows the profiles of  $\Omega$ ,  $v_R$  and  $H$  of the solution corresponding to  $\Omega_* = 0$ . This solution looks rather similar to the supersonic solution of Figure 1, except that it is entirely subsonic. A plot of  $H/R$  versus  $\Omega_*$  for various  $j$  is shown in Figure 8. Again,

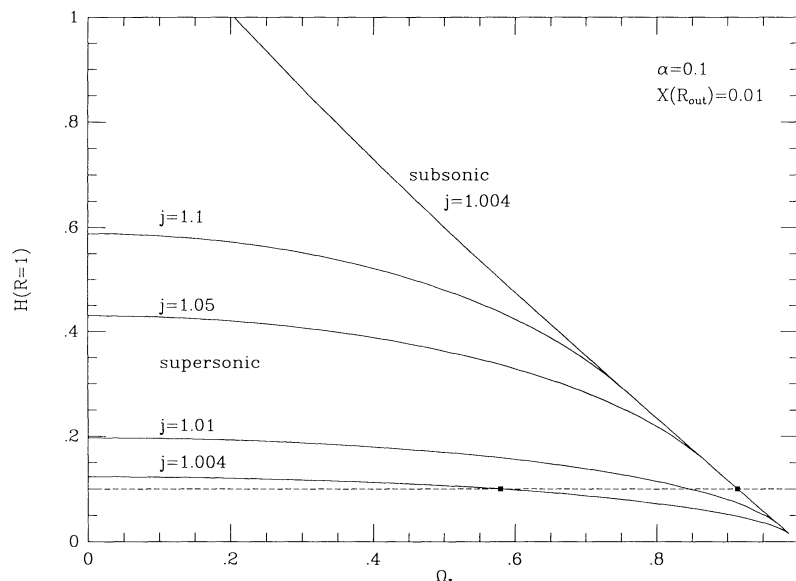


FIG. 4.—The disk height at the stellar surface  $H(R = 1)$  as a function of the stellar rotation rate  $\Omega_*$  for supersonic and subsonic solutions for  $X = 0.01$ ,  $\alpha = 0.1$ ,  $R_{\text{out}} = 100$ , and various values of  $j$ . For  $j > 1.0005$ , both supersonic and subsonic branches of solutions exist; the two branches meet at a cusp point, which moves to lower  $\Omega_*$  and higher disk height for larger values of  $j$ . For  $j < 1.0005$ , only subsonic solutions exist; the solutions corresponding to different  $j$  are very close together and are not resolved in this diagram.

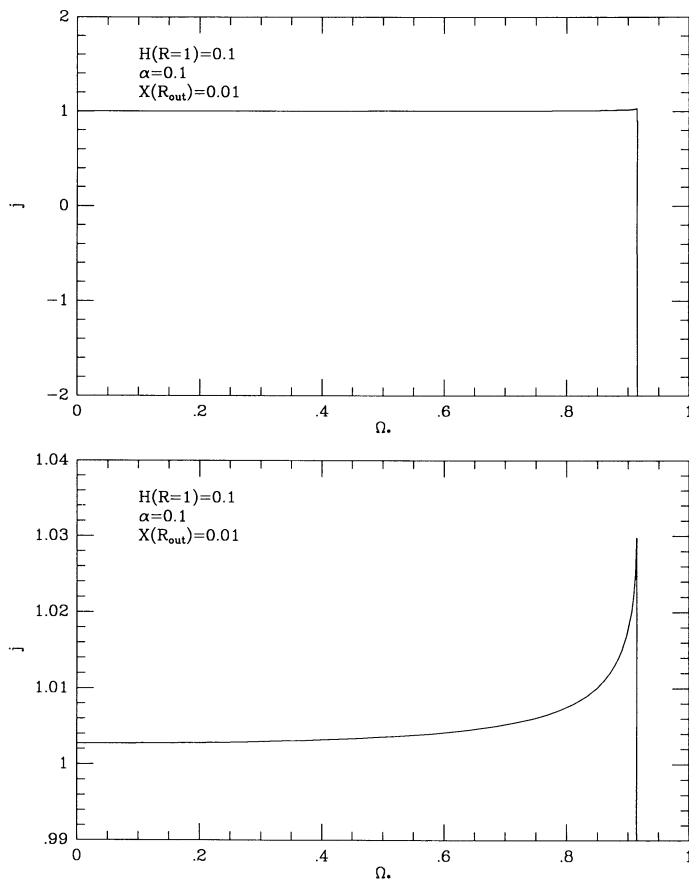


FIG. 5.—The variation of the specific angular momentum  $j$  with the stellar rotation rate  $\Omega_*$  for  $X = 0.01$ ,  $\alpha = 0.1$ ,  $R_{\text{out}} = 100$ , and our inner boundary condition,  $H(R = 1) = 0.1$ . The scale is expanded in the lower panel. For  $\Omega_* < 0.914$ , the solutions are supersonic and  $j \sim 1$ , as in the standard picture of a disk and boundary layer. The specific angular momentum is  $j \simeq 1.003$  at  $\Omega_* = 0$  and increases very slowly with  $\Omega_*$ , then more rapidly until it peaks at  $j \simeq 1.03$  at  $\Omega_* = 0.914$ . The peak in  $j$  corresponds to the transition between supersonic and subsonic solutions. Note that these values are expressed in our dimensionless units; the physical  $j$  actually increases more rapidly with  $\Omega_*$  due to rotational flattening of the star. For  $\Omega_* > 0.914$ , the solutions are subsonic, and  $j$  decreases very rapidly for only a slight increase in  $\Omega_*$ .

rather surprisingly, this looks quite similar to Figure 4, except that whereas there is a true cusp connecting the two branches in Figure 4, there is a rounded transition in Figure 8. The similarity between Figures 4 and 8 means that the mapping between  $j$  and  $\Omega_*$  in the present case will be very similar to the behaviour shown in Figure 5. We thus conclude that the main results of this paper are valid for quite a wide range of the disk thickness parameter  $X$  and viscosity parameter  $\alpha$ . The occurrence of supersonic solutions for astronomically relevant ranges of  $X$  and  $\alpha$  is quite interesting, but is not crucial to the argument.

#### 4. DISCUSSION

The main result of this paper is that we have found a branch of accretion disk solutions that transfer little, no, or even negative amounts of, angular momentum to the accreting star. These fully subsonic disk configurations (e.g., Figs. 2 and 6) are available whenever the star spins at a rate near its “breakup” rate,  $\Omega_{\text{max}}$ . Thus, by selecting the solution with the appropriate  $j$ , a rapidly rotating star can continue to accrete without spin-

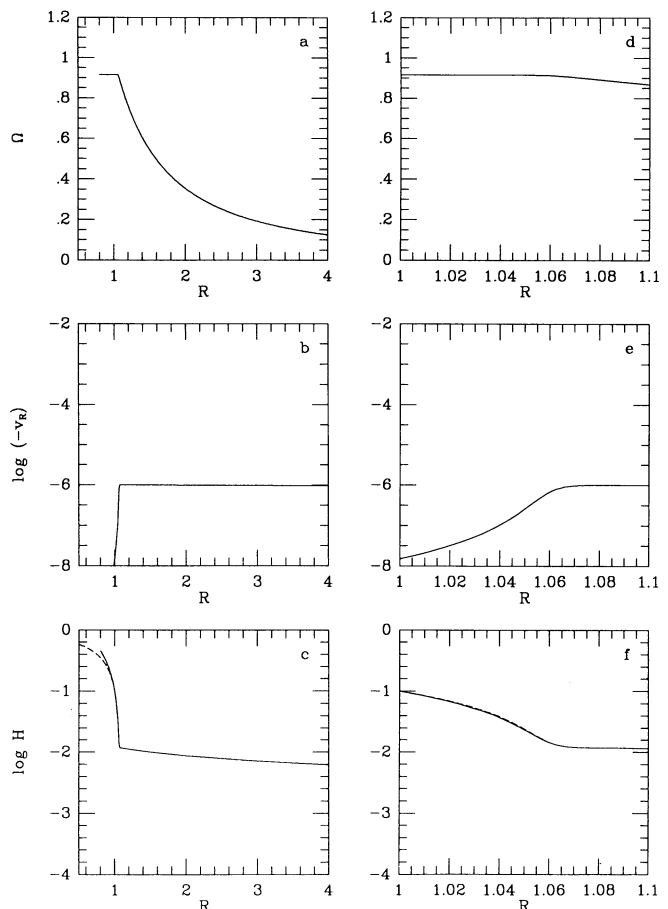


FIG. 6.—(a–f)  $\Omega$ ,  $v_R$ , and  $H$  for a subsonic disk solution corresponding to  $X = 0.01$ ,  $\alpha = 0.1$ ,  $R_{\text{out}} = 100$ ,  $j = -10$ , and  $\Omega_* = 0.915$ . Note the close similarity to the solution of Fig. 2 which corresponds to a more standard angular momentum accretion rate of  $j = 1.004$ ; as in Fig. 2, all quantities are continuous, and the dashed line shows  $H$  vs.  $R$  for a uniformly rotating star in a point-mass potential with the same  $\Omega_*$ .

ning up any further. The star thus achieves an “equilibrium” spin rate,  $(\Omega_*)_{\text{max}}$ . This is possible even in the extreme case of an accreting massive white dwarf, which has to *lose* angular momentum in order to accrete mass.

We have not been able to calculate precisely the ratio of the maximum or “equilibrium” spin rate,  $(\Omega_*)_{\text{max}}$ , to the “breakup” spin rate,  $\Omega_{\text{max}}$ . This question is discussed in § 3.3. The problem is that  $\Omega_{\text{max}}$  can be estimated only if the outer edge of the star can be identified, and we have been unable to do this in a unique way. For most of the calculations, we have defined the edge of the star to be the point at which the vertical half-thickness of the fluid is 1/10 of the radius. This arbitrary choice is quite adequate for most of the purposes of this paper, but it fails to provide an estimate of  $\Omega_{\text{max}}$ . Using a polytropic stellar model to define  $\Omega_{\text{max}}$ , it could be argued that the “equilibrium” spin rate  $(\Omega_*)_{\text{max}}$  exceeds breakup. Of course, the star is saved from actually breaking up because it rotates differentially on the outside, where it merges with the disk. In the discussion below we ignore the question of whether  $(\Omega_*)_{\text{max}}$  is greater or less than  $\Omega_{\text{max}}$ , and refer to the branch of solutions under discussion as merely being “near” breakup.

The wide range of  $j$  allowed in the solutions near breakup may seem paradoxical, but is actually easily understood. As



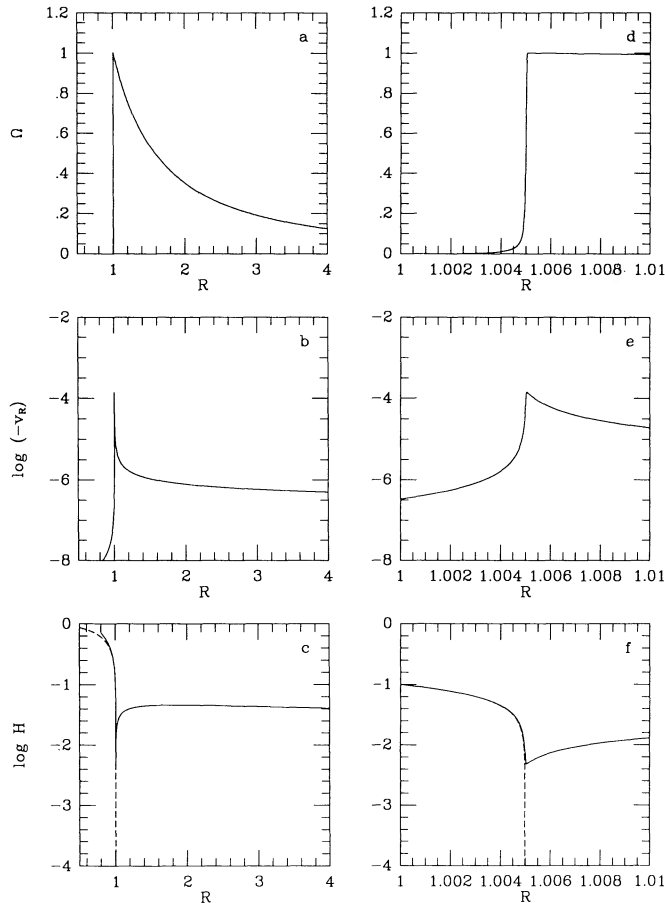


FIG. 7.—(a–f)  $\Omega$ ,  $v_R$ , and  $H$  for a subsonic disk solution corresponding to  $X = 0.1$ ,  $\alpha = 0.0001$ ,  $R_{\text{out}} = 100$ ,  $j = 1.0110$ , and  $\Omega_* = 0$ . Note the broad similarity to the supersonic solution of Fig. 1, except that this solution does not have a sonic point or shock, and there are no discontinuities in the quantities or their derivatives. The dashed line shows  $H$  vs.  $R$  for a uniformly rotating star in a point-mass potential with the same  $\Omega_*$ .

shown by equation (9), at any  $R$  in the disk there is angular momentum flow in opposite directions due to different causes. Angular momentum is advected inward by the accreting fluid, but at the same time angular momentum is also moved outward by shear stresses. The net flow,  $\dot{J} = j\dot{M}$ , is the difference of these two quantities, and can, in principle, have either sign and a range of magnitudes. There is a constraint, however, if the central star is rotating slowly. In that case,  $\Omega(R)$  must reach a maximum somewhere close to the stellar surface, so that  $d\Omega/dR = 0$ , and the shear stress vanishes (see Figs. 1 and 7). Consequently,  $\dot{J}$  is directly equal to the advected angular momentum at this radius and is constrained to be positive. Indeed, since the transition zone (the boundary layer) is usually narrow and occurs just outside the stellar surface, the value of  $j$  is constrained to have a value  $\sim 1$  (in our units). In contrast, the solutions that match on to a rapidly rotating star are very different. Here,  $d\Omega/dR < 0$  at all  $R$  and so there is an outward shear-induced flow of angular momentum at every point. By adjusting  $\Sigma(R)$  [or equivalently  $v_R(R)$  through eq. (3)], the outward angular momentum flow can be made larger or smaller than the advected flow, and so there is no constraint on either the magnitude or sign of  $\dot{J}$ .

An important feature of the solutions near breakup is that

there is a smooth transition from a near-Keplerian thin disk to the rapidly rotating star. Consequently, there is no separate entity such as a “boundary layer” separating the two; in particular, there is no component of additional luminosity from the boundary layer. It has been a long-standing problem that most cataclysmic variables show no evidence for the strong X-ray emission expected from the boundary layer (e.g., Ferland et al. 1982). It is tempting to speculate that most of these systems may be spinning near breakup and therefore no longer have distinct boundary layers.

In an earlier paper (Narayan & Popham 1989) we had argued against the accretion-induced-collapse (AIC) scenario for the formation of binary neutron stars, on the grounds that a white dwarf that has been spun up close to breakup will be unable to accrete any further. As we have shown in the present paper, this argument is false, and AIC is not limited by any barrier due to angular momentum. Also, although the winds and outflows produced by protostars may arise in the boundary-layer region, there is no necessity for such winds because of any barrier to accretion, as proposed by Shu et al. (1988).

The second branch of solutions that we have discovered corresponds to slowly rotating stars, with  $\Omega_*$  ranging from zero to a little below breakup. These solutions agree more closely with the standard picture of thin accretion disks (see Figs. 1 and 7). They have a narrow transition zone just outside the star where  $\Omega(R)$  falls rapidly from nearly Keplerian to nearly the stellar rate  $\Omega_*$ . A substantial fraction of the total luminosity of the system is produced in this boundary layer. In these solutions, the specific angular momentum accreted by the star corresponds to  $j \sim 1$ , as in the standard picture, and this value is only weakly dependent on  $\Omega_*$  (see Fig. 5).

An interesting feature of this branch of solutions is that the flow may or may not become supersonic close to the star, depending on the parameters of the disk. If the inequality of equation (19) is satisfied, the flow remains entirely subsonic, but if it is violated, the flow must become supersonic at least for some range of  $\Omega_*$ .

Standard disk parameters corresponding to cataclysmic variables, viz., relative disk thickness  $X \sim 0.01$ , viscosity parameter  $\alpha \sim 0.1$ , violate the condition (19) by a large factor, and so supersonic flow is indicated in these systems. We note that Kley (1989) also obtained supersonic flow in a two-dimensional calculation of a boundary layer including radiation processes. Rather surprisingly, the character of the mapping between  $j$  and  $\Omega_*$  does not seem to depend on whether the flow is subsonic or supersonic (see § 3.4). In those cases where there is supersonic flow, there is also a radial shock where most of the kinetic energy of free-fall is thermalized. The existence of this shock may possibly be identified observationally, thus providing a diagnostic to distinguish between subsonic and supersonic boundary layers.

We must mention, however, a potentially serious problem with the supersonic solutions. Since the supersonic zone between  $R_s$  and  $R_{sh}$  in these solutions acts like an isolating element between the star and the disk, no sound waves can travel back to the disk across the supersonic zone to convey information about the accreting star, and one wonders how the disk will adjust  $j$  in order to match the inner boundary condition. A resolution of this question is beyond the scope of the present analysis. However, we note that, within the assumptions of our analysis, and for reasonable choices of  $X$  and  $\alpha$  and a wide range of stellar rotation rates  $\Omega_*$ , the supersonic solu-



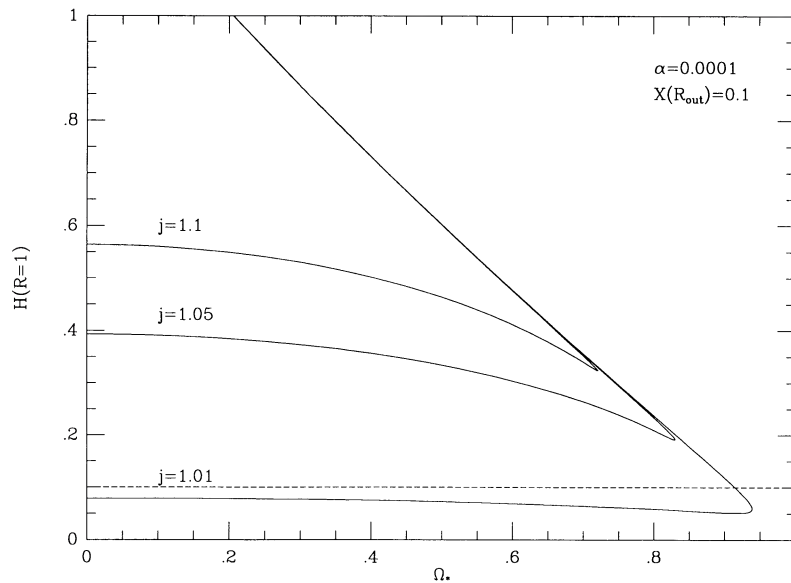


FIG. 8.—Similar to Fig. 4, but for  $X = 0.1$ ,  $\alpha = 0.0001$ ,  $R_{\text{out}} = 100$ . All the branches here are subsonic, in contrast to the case in Fig. 4, and the sharp cusps of Fig. 4 are rounded off here.

tions are the only ones that are allowed—there just are no other solutions that can match all the boundary conditions.

As we saw in § 3.4, the supersonic solutions can be avoided by reducing  $\alpha$  significantly and using a large value of  $X$ . We do not consider this alternative particularly attractive since our choice of these parameters is quite reasonable according to standard disk models (although Papaloizou & Stanley [1986] make the plausible argument that the boundary layer is likely to have a much smaller effective  $\alpha$  than the rest of the disk.) Another possibility is that the disk may violate either the steady state or axisymmetric assumptions. It is conceivable that a time-variable or nonaxisymmetric (e.g., spiral shocks, see Spruit 1987) solution may contrive to match the boundary conditions while at the same time remaining radially subsonic.

Any such solution will, in a time/azimuthally averaged sense, probably be similar to our supersonic solutions.

It seems likely that the spectra of accretion disks around rapidly rotating stars, particularly disks with negative  $j$ , will be different from the spectra of standard models of thin disks. In order to calculate realistic spectra for comparison with observations one should solve a more complete set of equations than we have done here, including an energy equation and radiative transfer. We are currently working on this.

It is a pleasure to acknowledge fruitful discussions with B. Paczyński and J. E. Pringle. This work was supported by a National Science Foundation Presidential Young Investigator award to RN (grant No. AST-8957101).

## APPENDIX A

### POLYTROPIC FLUIDS

#### 1. TWO-DIMENSIONAL FLUID

We assume that the height-integrated two-dimensional fluid has an equation of state of the form

$$P = K\Sigma^\gamma, \quad (\text{A1})$$

where  $K$  and  $\gamma$  are constants. This leads to a relation between the two-dimensional sound speed,  $c_s$ , and the radial infall velocity,  $v_R$ , (see eq. [4])

$$c_s^2 = \frac{dP}{d\Sigma} = C_0(R|v_R|)^{1-\gamma}, \quad (\text{A2})$$

where  $C_0$  is a constant.

Consider now the outer regions of the disk, where  $\Omega(R)$  is very nearly equal to the Keplerian  $\Omega_K(R) = (GM/R^3)^{1/2}$ . Further, assume that  $j/R^{1/2} \ll 1$ . Then, equations (3), (10), (11), and (A2), show that  $v_R$ ,  $\Sigma$  and  $c_s$  scale as follows with radius,

$$v_R \propto R^{-(2\gamma-3)/2\gamma}, \quad (\text{A3})$$

$$\Sigma \propto R^{-3/2\gamma}, \quad (\text{A4})$$

$$c_s \propto R^{-3(\gamma-1)/4\gamma}. \quad (\text{A5})$$

In the detailed theory of thin accretion disks, the regime of the “outer disk” is defined as the region where gas pressure dominates over radiation pressure and free-free opacity dominates over electron scattering (Shakura & Sunyaev 1973). In this regime it can be shown that  $v_R \propto R^{-1/4}$ ,  $\Sigma \propto R^{-3/4}$  (see e.g., Frank, King, & Raine 1985). We see that we can simulate this dependence with our two-dimensional fluid by choosing

$$\gamma = 2. \quad (\text{A6})$$

Since most accretion disks do have an extended “outer disk,” we specialize to this value of  $\gamma$  in all our calculations. We thus hope to obtain “realistic” behavior over at least some part of our simulated fluid.

## 2. THREE-DIMENSIONAL FLUID

Let the fluid have a three-dimensional equation of state of the form

$$P_3 = K_3 \rho^{\gamma_3}, \quad (\text{A7})$$

where  $P_3$  is the pressure,  $\rho$  is the density,  $\gamma_3$  is assumed to be constant, and  $K_3$  is in general a function of  $R$ . Vertical hydrostatic equilibrium requires

$$\frac{GMz}{(R^2 + z^2)^{3/2}} = -\frac{1}{\rho} \frac{\partial P_3}{\partial z} = -\frac{K_3 \gamma_3}{\gamma_3 - 1} \frac{d(\rho^{\gamma_3 - 1})}{dz} \quad (\text{A8})$$

where  $M$  is the mass of the central star. Integrating, and writing the result in terms of the Keplerian frequency,

$$\Omega_K(R) = \sqrt{GM/R^3}, \quad (\text{A9})$$

we have

$$\rho(z) = \left[ \frac{(\gamma_3 - 1)\Omega_K^2}{2K_3 \gamma_3} (H^2 - z^2) \right]^{1/(\gamma_3 - 1)}, \quad (\text{A10})$$

where  $H$  is the vertical half-thickness of the fluid, and we have assumed  $H \ll R$ . Similarly, we obtain

$$P_3(z) = K_3 \left[ \frac{(\gamma_3 - 1)\Omega_K^2}{2K_3 \gamma_3} (H^2 - z^2) \right]^{\gamma_3/(\gamma_3 - 1)}. \quad (\text{A11})$$

We now calculate the height-integrated surface density,  $\Sigma$ , and two-dimensional pressure,  $P$ , of the fluid:

$$\Sigma = \int_{-H}^H \rho(z) dz = \sqrt{\pi} \frac{\Gamma[\gamma_3/(\gamma_3 - 1)]}{\Gamma[(3\gamma_3 - 1)/2(\gamma_3 - 1)]} \left( \frac{\gamma_3 - 1}{2K_3 \gamma_3} \right)^{1/(\gamma_3 - 1)} \Omega_K^{2/(\gamma_3 - 1)} H^{(\gamma_3 + 1)/(\gamma_3 - 1)}, \quad (\text{A12})$$

$$P = \int_{-H}^H P_3(z) dz = \sqrt{\pi} \frac{\Gamma[(2\gamma_3 - 1)/(\gamma_3 - 1)]}{\Gamma[(5\gamma_3 - 3)/(\gamma_3 - 1)]} K_3 \left( \frac{\gamma_3 - 1}{2K_3 \gamma_3} \right)^{\gamma_3/(\gamma_3 - 1)} \Omega_K^{2\gamma_3/(\gamma_3 - 1)} H^{(3\gamma_3 - 1)/(\gamma_3 - 1)}. \quad (\text{A13})$$

If  $P$  and  $\Sigma$  are to have a polytropic relation as in equation (A1), then we require  $K_3$  to scale as

$$K_3 = K_0 \Omega_K^{2(\gamma - \gamma_3)/(\gamma - 1)} H^{(1 + \gamma - 3\gamma_3 + \gamma\gamma_3)/(\gamma - 1)}, \quad (\text{A14})$$

with  $K_0$  a constant. Substituting this in (A12) and (A13) we find

$$\Sigma = \sqrt{\pi} \frac{\Gamma[\gamma_3/(\gamma_3 - 1)]}{\Gamma[(3\gamma_3 - 1)/2(\gamma_3 - 1)]} \left( \frac{\gamma_3 - 1}{2\gamma_3 K_0} \right)^{1/(\gamma_3 - 1)} \Omega_K^{2/(\gamma - 1)} H^{2/(\gamma - 1)}, \quad (\text{A15})$$

$$P = \sqrt{\pi} \frac{\Gamma[(2\gamma_3 - 1)/(\gamma_3 - 1)]}{\Gamma[(5\gamma_3 - 3)/(\gamma_3 - 1)]} \left( \frac{\gamma_3 - 1}{2\gamma_3} \right) \left( \frac{\gamma_3 - 1}{2\gamma_3 K_0} \right)^{1/(\gamma_3 - 1)} \Omega_K^{2\gamma/(\gamma - 1)} H^{2\gamma/(\gamma - 1)}. \quad (\text{A16})$$

The two-dimensional sound speed then becomes

$$c_s^2 = \frac{dP}{d\Sigma} = \frac{\gamma(\gamma_3 - 1)}{(3\gamma_3 - 1)} \Omega_K^2 H^2; \quad \text{i.e., } \frac{c_s}{\Omega_K R} = \left[ \frac{\gamma(\gamma_3 - 1)}{(3\gamma_3 - 1)} \right]^{1/2} \frac{H}{R}. \quad (\text{A16})$$

This relation allows us to estimate the vertical thickness of the fluid in terms of the sound speed  $c_s$ .

The above relations are written for arbitrary  $\gamma$  and  $\gamma_3$ . We have already specified the value of  $\gamma$  in equation (A6). To fix  $\gamma_3$ , we need some other criterion. We decided that we would like  $K_3$  to be independent of  $H$  for given  $\Omega_K$ . This permits our fluid to behave like a star with a three-dimensionally polytropic equation of state in the transition region between the disk and the star. For  $\gamma = 2$ , this corresponds to

$$\gamma_3 = 3. \quad (\text{A17})$$

Equation (A16) then becomes

$$\frac{c_s}{\Omega_K R} = \frac{1}{\sqrt{2}} \frac{H}{R}. \quad (\text{A18})$$

This relation is used in the paper to estimate the vertical thickness of the fluid. Note that when equation (A18) is combined with equation (A5) we obtain a scaling of the form,

$$H/R \propto R^{1/8}, \quad (\text{A19})$$

a standard result for the regime of the outer accretion disk.

## APPENDIX B

### THE CONDITION FOR A SUBSONIC BOUNDARY LAYER

Although the following analysis can easily be done for an arbitrary  $\Omega_*$ , we will for simplicity assume  $\Omega_* = 0$ . For such a star, the boundary layer will occur at  $R \sim 1$ , and the disk solution will correspond to  $j \sim 1$ . Consider a subsonic boundary layer with  $v_R < c_s \ll \Omega_* R \sim 1$ . Under these conditions, equations (7), (10), and (11) simplify to

$$\frac{d|v_R|}{dR} \sim \frac{|v_R|(1 - \Omega^2)}{(c_s^2 - v_R^2)} > \frac{|v_R|(1 - \Omega^2)}{c_s^2}, \quad (\text{B1})$$

$$\frac{d\Omega}{dR} \sim \frac{|v_R|}{\alpha c_s^2} (1 - \Omega). \quad (\text{B2})$$

Combining these two equations, we find

$$\frac{d|v_R|}{d\Omega} > \alpha(1 + \Omega) > \alpha. \quad (\text{B3})$$

Now, in the boundary layer,  $\Omega$  increases from 0 to  $\sim 1$ . Therefore,  $|v_R|$ , which is extremely small inside the star, will have a value outside the boundary layer given approximately by

$$|v_R| \gtrsim \alpha. \quad (\text{B4})$$

The solution will be subsonic only if the above value of  $v_R$  is less than the sound speed. From equations (4) and (16), setting  $R \sim 1$  and assuming  $j/R_{\text{out}}^{1/2} \ll 1$ , we estimate the sonic  $|v_R|$  to be

$$|v_R|_{\text{sonic}} \sim C_0^{2/(\gamma+1)} \sim (3/2)^{(\gamma-1)/(\gamma+1)} R_{\text{out}}^{-(3-\gamma)/2(\gamma+1)} \alpha^{(\gamma-1)/(\gamma+1)} X^{2\gamma/(\gamma+1)}. \quad (\text{B5})$$

The condition for a subsonic boundary layer then becomes

$$\alpha < (3/2)^{(\gamma-1)/2} R_{\text{out}}^{-(3-\gamma)/4} X^\gamma. \quad (\text{B6})$$

For our particular choice of parameters,  $\gamma = 2$ ,  $R_{\text{out}} = 100$ , this gives

$$\alpha \lesssim 0.39 X^2. \quad (\text{B7})$$

An inspection of the sense of the inequalities in equations (B1) and (B3) shows that the coefficient in equation (B7) is likely to be an overestimate, possibly by a factor of  $\sim 2$ .

## REFERENCES

- Abramowicz, M. A., Czerny, B., Lasota, J. P., & Szuszkiewicz, E. 1988, *ApJ*, 332, 646  
 Ferland, G. J., Langer, S. H., MacDonald, J., Pepper, G. H., Shaviv, G., & Truran, J. W. 1982, *ApJ*, 262, L53  
 Frank, J., King, A. R., & Raine, D. J. 1985, *Accretion Power in Astrophysics*, (Cambridge: Cambridge University Press)  
 Ghosh, P., & Lamb, F. K. 1979, *ApJ*, 234, 296  
 Hachisu, I. 1986, *ApJS*, 61, 479  
 Kley, W. 1989, in *Theory of Accretion Disks*, ed. F. Meyer, W. J. Duschl, J. Frank, & E. Meyer-Hofmeister (Dordrecht: Kluwer Academic), 289  
 Lewin, W. H. G., & van den Heuvel, E. P. J., eds. 1984, *Accretion-driven Stellar X-ray Sources* (Cambridge: Cambridge University Press)  
 Muchotrzeb, B., & Paczyński, B. 1982, *Acta Astr.*, 32, 1  
 Narayan, R., & Popham, R. 1989, *ApJ*, 346, L25  
 Paczyński, B. 1990, preprint  
 Paczyński, B., & Bisnovatyi-Kogan, G. 1981, *Acta Astr.*, 31, 283  
 Papaloizou, J. C. B., & Stanley, G. Q. G. 1986, *MNRAS*, 178, 195  
 Press, W. H., Flannery, B. P., Teukolsky, S. A., & Vetterling, W. T. 1986, *Numerical Recipes* (Cambridge: Cambridge University Press)  
 Pringle, J. E. 1981, *ARA&A*, 19, 137  
 ———. 1989, *MNRAS*, 236, 107  
 Shakura, N. I., & Sunyaev, R. A. 1973, *A&A*, 24, 337  
 Shu, F. H., Lizano, S., Ruden, S. P., & Najita, J. 1988, *ApJ*, 328, L19  
 Spruit, H. C. 1987, *A&A*, 184, 173